

LA-UR- 98-3112

Approved for public release;
distribution is unlimited.

Title:

THERMAL ANALYSIS OF THE APT MATERIALS IRRADIATION SAMPLES

CONF-980921--

Author(s):

S. A. Maloy, G. J. Willcutt, M. R. James, J. Teague,
D. A. Diebe, W. F. Sommer, P. D. Ferguson

Submitted to:

ACC APP'98-Applications of Accelerator Technology
Gatlinburg, TN
Sept. 20-23/98

DISTRIBUTION OF THIS DOCUMENT IS UNLIMITED

MASTER

Los Alamos
NATIONAL LABORATORY



Los Alamos National Laboratory, an affirmative action/equal opportunity employer, is operated by the University of California for the U.S. Department of Energy under contract W-7405-ENG-36. By acceptance of this article, the publisher recognizes that the U.S. Government retains a nonexclusive, royalty-free license to publish or reproduce the published form of this contribution, or to allow others to do so, for U.S. Government purposes. Los Alamos National Laboratory requests that the publisher identify this article as work performed under the auspices of the U.S. Department of Energy. The Los Alamos National Laboratory strongly supports academic freedom and a researcher's right to publish; as an institution, however, the Laboratory does not endorse the viewpoint of a publication or guarantee its technical correctness.

DISCLAIMER

This report was prepared as an account of work sponsored by an agency of the United States Government. Neither the United States Government nor any agency thereof, nor any of their employees, makes any warranty, express or implied, or assumes any legal liability or responsibility for the accuracy, completeness, or usefulness of any information, apparatus, product, or process disclosed, or represents that its use would not infringe privately owned rights. Reference herein to any specific commercial product, process, or service by trade name, trademark, manufacturer, or otherwise does not necessarily constitute or imply its endorsement, recommendation, or favoring by the United States Government or any agency thereof. The views and opinions of authors expressed herein do not necessarily state or reflect those of the United States Government or any agency thereof.

DISCLAIMER

**Portions of this document may be illegible
in electronic image products. Images are
produced from the best available original
document.**

THERMAL ANALYSIS OF THE APT MATERIALS IRRADIATION SAMPLES

S.A. Maloy, G.J. Willcutt, M.R. James, J. Teague, D.A. Siebe, W.F. Sommer, P.D. Ferguson
 Materials Science and Technology Division
 Los Alamos National Laboratory
 Box 1663, MS H 805
 Los Alamos, New Mexico 87545

Introduction

The accelerator production of tritium (APT) project proposes to use a 1.7 GeV, 100 mA proton beam to produce neutrons from an Inconel 718 clad tungsten target. The neutrons are multiplied and moderated in a lead/water blanket before being captured in He^3 to form tritium. In this process, the materials in the target and blanket region are exposed to a wide range of different fluxes comprised of protons and neutrons with energies into the GeV range. To investigate the effect of irradiation on the mechanical properties of candidate APT materials (Inconel 718, 316L stainless steel, Al 6061-T6, Mod 9Cr-1Mo, 304L stainless steel and Al5052-0), the APT Engineering Design and Development group fielded an extensive materials irradiation using the LANSCE (Los Alamos Neutron Science Center) accelerator, which operates at an energy of 800 MeV and a current of 1 mA. The test set-up was designed to place mechanical test specimens in locations in and near the proton beam where the environment of proton and neutron fluxes and temperatures are prototypic to those expected in the APT target/blanket (50-170°C). After irradiating for about 3600 hours, the maximum achieved proton fluence was $4.5 \times 10^{21} \text{ p/cm}^2$ for the materials in the center of the beam.

To obtain relevant data on the change in the mechanical properties with fluence, it is essential to know the temperature at which the materials were irradiated. In this test, specimens were placed in sandwiches made of two cover plates and a central spacer which were stacked together in tubes and centered in the proton beam. Determining the temperature of specimens in these sandwiches was based on three essential steps. First, local power densities were determined at specific locations in the irradiation using the Los Alamos High Energy Transport (LAHET) Code System. Second, the

temperature in each tube is measured by three thermocouples placed in one sandwich between cover plates. Third, a thermohydraulic calculation is performed to determine the gap resistance between the thermocouple and the cover plate using the local power densities determined in the first step. These calculated gap resistances are then used to determine the temperature of the specimens during the irradiation. The following sections will explain the method of determining the specimen temperature and report some specific examples.

Procedure-
Experimental Set-up

The specimen irradiation was performed at the Los Alamos Spallation Radiation Effects Facility (LASREF) at LANSCE. This facility was used to irradiate capsules using an 800 MeV, 1mA proton beam (with a Gaussian distribution where 2 sigma is 3 cm). Capsules are placed at the end of 12 ft. long steel shielding inserts. Water

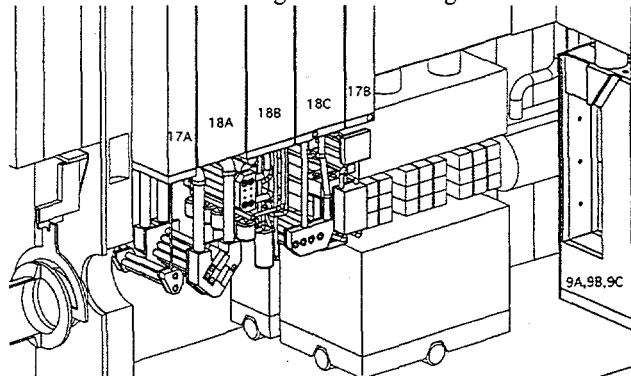


Figure 1 Close-up of the arrangement of capsules used to expose samples and prototype components to a spallation source radiation environment.

cooling lines and thermocouples travel down grooves on the sides of the inserts to measure temperature and provide water cooling to the capsule during the irradiation. The set-up of the five capsules irradiated for 3600 hours from Sept.-Nov. 1996 and March-July 1997 is shown in Figure 1. The five capsules are referred to as 17A, 18A, 18B, 18C and 17B. Capsule 17A holds specimens which are irradiated with the pure highest power proton beam. These specimens are placed in sandwiches and stacked in tubes as previously described. Capsule 18A is the tungsten neutron source. The tungsten is in the form of 0.264 cm (0.104 in.) diameter rods clad in 0.318 cm (0.125 in.) outer diameter 304L stainless steel. There are 19 rods in each of ten tubes with 4 tubes on beam centerline, a row of three tubes above beam centerline, and another row of three tubes below beam centerline. Capsule 18B holds specimens for other specialized tests. Capsule 18C contains 12 tubes; 9 hold specimens in sandwiches and 3 hold clad tungsten rod bundles. The temperature calculation described in this paper directly pertains to the specimens in this capsule. Capsule 17B contains specimens used for corrosion measurements. For a more detailed description of these capsules see reference 1.

Specimens were placed in sandwiches in tubes using two different arrangements depending on the thermocouples used. One arrangement (arrangement A) used sheathed 0.031 in. diameter type K thermocouples. A second arrangement (arrangement B) used sheathed 0.062 in. diameter type K thermocouples.

A cross section of the sandwich set-up for arrangement A is shown in Fig. 2a. In this arrangement, eight sandwiches are equally spaced 0.031 in. apart with a stainless steel wire. All cover plates and holders for each sandwich were made of 304L stainless steel. Each sandwich consists of a center spacer and a 0.010 in. thick cover plate on each side. A plan view of the center spacers used in arrangement A is shown in Fig. 3. Sandwiches 1 and 8 hold 19 TEM disks ($t=0.25$ mm). Sandwich 2 holds two layers of 21 TEM disks. Sandwiches 3, 4 and 6 hold 12 S-1 tensile ($t=0.25$ mm) and 48 bend (2 mm x 8 mm, $t=0.25$ mm) specimens stacked on top of each other. Sandwich 5 holds 6 compact tension specimens ($t=2.0$ mm) and 7 stacks of activation foils. Sandwich 7 holds 6 S-1 tensile ($t=0.75$ mm) and 24 bend (2 mm x 8 mm, $t=0.75$ mm) and three thermocouples brazed in metal pads.

A cross section of the sandwich set-up for arrangement B is shown in Fig. 2b. In this arrangement, seven sandwiches are equally spaced in the tube 0.031 in. apart with a stainless steel wire. Each sandwich consists of a center spacer and two 0.010 in. thick cover plates on each side. A plan view of the center spacers used in arrangement B is shown in Fig. 4. Sandwiches 1 and 7 hold 19 TEM disks ($t=0.25$ mm). Sandwich 2 holds two

layers of 21 TEM disks. Sandwich 3 holds three thermocouples spaced as shown. This sandwich uses 0.020 in. thick cover plates. Sandwich 4 holds 6 compact tension specimens ($t=2.0$ mm) and 7 stacks of activation foils. Sandwiches 5 hold 12 S-1 tensile ($t=0.25$ mm) and 48 bend (2 mm x 8 mm, $t=0.25$ mm) specimens stacked on top of each other and sandwich 6 holds 12 S-1 tensile ($t=0.75$ mm) and 48 bend (2 mm x 8 mm, $t=0.75$ mm) specimens stacked on top of each other. For a more detailed description of the specimens mentioned above see ref. 2.

Physics Calculation

The LAHET code system was used to calculate power densities for the sample materials, holders and cover plates, and tube wall for each of the nine sample tubes in capsule 18C. An important input needed for this calculation is the actual position of the capsules relative to the beam position. This was determined by performing autoradiography on one sandwich from each tube after the irradiation. For capsule 17A, the capsule was shifted 1.27 cm (0.5 in.) upward and was on the beam centerline in the horizontal direction. For the tungsten neutron source capsule 18A, the capsule was centered vertically and shifted 1.3 cm (0.52 in.) to the south. For the capsule 18C, the capsule was shifted upward 0.89 cm (0.35 in.) and shifted horizontally 1.0 cm (0.39 in.) to the south. The power densities include the effects of the protons, neutrons, and photons. For each tube, a representative sample material for the seven or eight sample sandwiches is modeled as one thick sandwich with the center representing a composite of all of the samples and the two sides representing a composite of all of the holders and cover plates. Power densities are determined at twenty-one node locations along the 15.88 cm (6.25 in.) holder length with finer detail near the center of the beam.

A separate post processor model was used to calculate power density averages and distributions from the power density input determined by the LAHET calculations. For each tube, the ratio of sample power density at each of 21 nodes to the average was determined for the entire tube length. Power densities are also determined in the manifolds. These average and ratio to average power densities at each node are used as input in the detailed sample temperature calculations to determine local power densities.

Because all materials are not modeled in the physics model, the electron density of the materials for which power density is not known is used to scale from the LAHET calculated sample power density in each tube. Electron density equals atomic number times atom density. Note the physics calculations calculate power densities for one representative sample material per tube. Electron density scaling is used to calculate the power densities in the other sample materials in the tube.

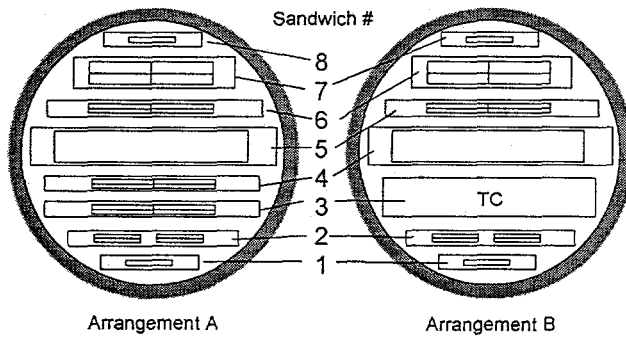


Figure 2 Diagram showing arrangement of sandwiches in water coolant tube.

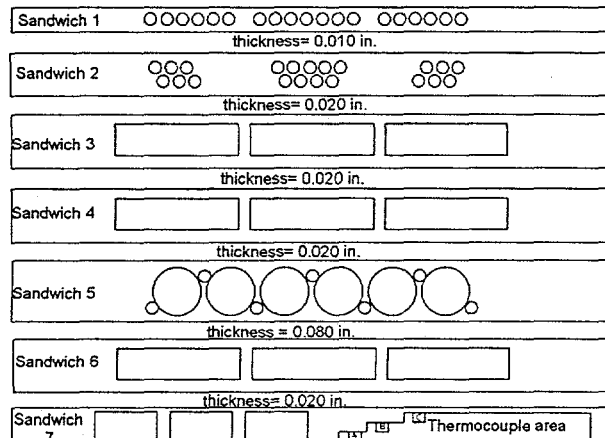


Figure 3 Diagram showing plan view of sandwich centers in arrangement A.

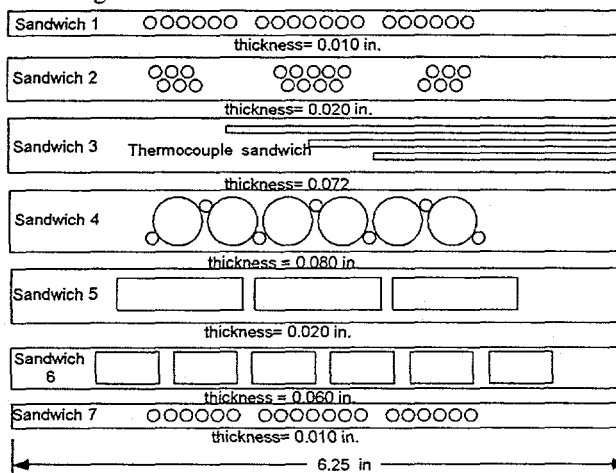


Figure 4 Diagram showing plan view of sandwich centers in arrangement B.

Determining water temperature

The water inlet temperature to capsule 18C was 28 °C, and the measured flow rate to the nine sample tubes in series was 8 gpm. There is approximately 1.93 kW deposited in the flow manifolds at each end of the tubes. This power was assumed to be deposited in the water before entering the first tubes of each circuit so the inlet was adjusted to 28.29 °C. Next, to determine the increase in water temperature at each node one must determine the contribution from power deposited in the water and power deposited in the sandwiches on each side of the channel. The water temperature increase from the power deposited in the water is just the power added to the water divided by the product of the mass flow rate times specific heat. The temperature increase from the power deposited in the sandwiches on each side of the channel equals the power in the cover plate plus half the power in the samples plus holder. Each is determined from their respective power density times volume. Then, for each successive tube the inlet temperature was increased by the power deposition in the water from the previous tube as shown in the Table 1.

Table 1 Water Inlet Temperature to Each Tube

Flow Direction Sequence No.	Tube Number	Total Power in Tube (kW)	Water Temp. Increase (C)	Inlet Temp to Tube (C)
1	23	2.36	1.13	28.29
2	21	4.10	1.96	29.41
3	22	4.40	2.10	31.37
4	24	4.16	1.99	33.47
5	25	4.33	2.07	35.46
6	28	3.85	1.84	37.53
7	27	3.84	1.83	39.37
8	29	2.34	1.12	41.20
9	26	2.50	1.19	42.32

Models for calculating Sample temperatures

One model calculates the detailed temperature distributions for one tube containing eight sets of sample sandwiches for Arrangement A. Each sandwich consists of a center plate with specimens in it and cover plates on each side. Tube flow rate, inlet pressure, and inlet water temperature, T_{water} , are provided as boundary conditions. To begin the calculation, one must know the following information:

q_s and q_{cp} , the heat generation in the cover plate and sample, determined from the LAHET calculation; Δx and Δx_s , the thickness of the sample and the cover plate; k_s and k_{cp} , the conductivity of the sample and the cover plate and, R_{gap} , the gap resistance between the sample and the cover plate.

Next the heat flux out of the sample Q_s and the cover plate, Q_{cp} , are determined from the following formulas:

$$Q_s = \frac{q_s \Delta x_s}{2}; Q_{cp} = Q_s + q_{cp} \Delta x_{cp}$$

Then, at each node the peak temperature in the sample is calculated in a series of steps including the temperature difference in the sample, ΔT_{sam} , the temperature difference across the gap between the sample and cover plate ΔT_{gap} , the temperature difference in the cover plate ΔT_{cov} and the film drop between the cover plate surface and the bulk water temperature, ΔT_{film} using the following calculations:

$$\Delta T_{sam} = \frac{q_s \Delta x_s^2}{8k_s}; \Delta T_{gap} = Q_s R_{gap}$$

$$\Delta T_{cov} = \frac{q_{cp} \Delta x_{cp}^2}{2k_{cp}} + \frac{Q_s \Delta x_{cp}}{k_{cp}}; \Delta T_{film} = \frac{Q_{cp}}{H}$$

From this information, the temperature on the outer cover surface, T_{OCS} , the temperature on the inner cover surface, T_{ICS} , the temperature on the sample surface, T_{ss} and the peak sample temperature, T_{sp} can be determined as follows:

$$T_{OCS} = T_{water} + \Delta T_{film}; T_{ICS} = T_{OCS} + \Delta T_{cov}$$

$$T_{ss} = T_{ICS} + \Delta T_{gap}; T_{sp} = T_{ss} + \Delta T_{sam}$$

These detailed calculations are then used to determine sample temperatures at 21 node locations in each sandwich in the tube. Calculations are done for 7 channels between the eight sandwiches and two more between the outer sandwich and the tube wall. A second modified model does the similar calculations for the Arrangement B tube with seven sets of sample sandwiches.

Determining Gap Resistance

The gap resistance between the cover plate and the specimen is a critical value for determining the specimen irradiation temperature. These gap resistances were

determined by calculating the gap resistance needed at each thermocouple location to match the calculated temperature with thermocouple measurements. Initial temperatures and heat fluxes are calculated for each node location using the two models, but using zero gap resistance. This is done for all six tubes with arrangement B and three tubes with arrangement A. The temperatures and heat fluxes are then interpolated from the nodes nearest the thermocouple locations to determine the calculated temperature and heat flux at each thermocouple location. The gap resistance between the sample holder (thermocouple holder) and the cover plate is then calculated that gives the same calculated and measured thermocouple temperature. The nominal gap resistance used, $4.5 \times 10^{-5} \text{ m}^2 \text{ C/W}$ is based on this range of calculated gap resistances that matches the thermocouple and calculated value at each location.

Table 2 shows the gap resistance needed at each thermocouple location to match the calculated and measured thermocouple temperatures. Tubes 21 through 26 have the 1/16 in. thermocouples that are brazed into a groove in the holder plate as shown in Fig. 4. Tubes 27 through 29 have the 1/32 in. thermocouples that are held in pads between the cover plates as shown in Fig. 3. The 1/32 in. thermocouple design was judged to be more accurate in predicting contact resistances to be applied to all of the sample locations because there is less possibility of heat flow laterally in the holder with the pad design. The nominal value of $4.5 \times 10^{-5} \text{ m}^2 \text{ C/W}$ was based on tubes 27 and 28, because there was a problem with the data for tube 29 that gave much higher values than at any other location containing either type of thermocouple. The expected variation in the nominal value based on all of the data except that from tube 29 is about a factor of

Table 2 Gap Resistances to Match Thermocouple Temperatures at Each Location

Tube	Thermocouple A ($\times 10^{-5} \text{ m}^2 \text{ C/W}$)	Thermocouple B ($\times 10^{-5} \text{ m}^2 \text{ C/W}$)	Thermocouple C ($\times 10^{-5} \text{ m}^2 \text{ C/W}$)
21	2.727	5.920	7.454
22	2.216	8.763	4.846
23	4.320	8.435	2.529
24	2.577	8.260	5.348
25	0.6908	4.667	2.179
26	6.796	10.47	9.309
27	4.460	4.478	4.612
28	3.900	4.512	1.917
29	11.78	13.65	17.12
Avg 21 to 26	3.221	7.753	5.278
Avg 27 to 28	4.180	4.495	3.265

Table 3 Peak Temperatures in Each Sample Sandwich in Higher Power Tube 22

Sandwich Number	Description	Material	Peak Temp. (C)
1	1 layer of TEM disks	304L SS	41.9
2	2 layers of TEM disks	304L SS	48.1
3	3 large thermocouples	Braze	92.3
4	1 layer of compact tension samples	304L SS	91.3
5	2 layers of thin tensile or bend	304L SS	48.0
6	2 layers of thick tensile or bend	304L SS	74.5
7	1 layer of TEM disks	304L SS	42.0

Table 4 Peak Temperatures in Each Sample Sandwich in Lower Power Tube 23

Sandwich Number	Description	Material	Peak Temp. (C)
1	1 layer of TEM disks	Modified 9 Cr-1 Mo	33.2
2	2 layers of TEM disks	Modified 9 Cr-1 Mo	36.0
3	3 large thermocouples	Braze	56.4
4	1 layer of compact tension samples	Modified 9 Cr-1 Mo	53.7
5	2 layers of thin tensile or bend	Modified 9 Cr-1 Mo	35.9
6	2 layers of thick tensile or bend	Modified 9 Cr-1 Mo	47.0
7	1 layer of TEM disks	304L SS	33.3

two over the nominal. Most of the data lies within this $9.0 \times 10^{-5} \text{ m}^2 \text{C/W}$ value of the nominal plus expected variation.

Table 5 Peak Temperatures in Tube 27 with 8 Sample Sandwiches

Sandwich Number	Description	Material	Peak Temp. (C)
1	1 layer of TEM disks	304L SS	48.1
2	2 layers of TEM disks	Aluminu m 6061	46.4
3	2 layers of thin tensile or bend	Aluminu m 6061	46.5
4	2 layers of thin tensile or bend	316L SS	53.0
5	1 layer of compact tension samples	Inconel 718	91.8
6	2 layers of thin tensile or bend	316L SS	53.0
7	2 layers of thick tensile or bend	Modified 9 Cr-1Mo	72.0
8	1 layer of TEM disks	304L SS	48.2

Results of Temperature Calculations

Tables 3-5 show peak temperatures for each of seven sample sandwiches in tube 22, where the beam power is highest, tube 23 with seven sample sandwiches that has lower beam power, and tube 27 that is an example of a tube with sandwiches in arrangement A.

Table 6 shows the peak temperature in the compact tension samples for each tube. As an example, the contributions to peak temperature in the compact tension samples in tube 22 are as follows. The water temperature at that location is 33.5 C. The temperature rise from the bulk water temperature to the cover plate surface is 17.7 C; there is a 7.5 C rise through the cover plate from the power density in the cover plate plus the power removed through the cover plate from the compact tension samples; there is a 19.2 C rise across the gap resistance between the cover plate and sample holder; and there is a 13.4 C temperature rise from the surface of the compact tension sample to the centerline. This gives a peak temperature in the compact tension sample of 91.3 C.

Figure 5 shows the variation of center temperature in the compact tension samples in Tube 22 with location. The shift of the capsule relative to the beam is evident.

Table 6 Peak Temperatures in Compact Tension Samples

Tube Number	Compact Tension Material	Peak Temp. (C)
21	Inconel 718	88.4
22	304L SS	91.3
23	Modified 9 Cr-1 Mo	53.7
24	316L SS	84.9
25	Modified 9 Cr-1 Mo	83.1
26	304L SS	71.1
27	Inconel 718	91.8
28	Modified 9 Cr-1 Mo	80.5
29	316L SS	67.6

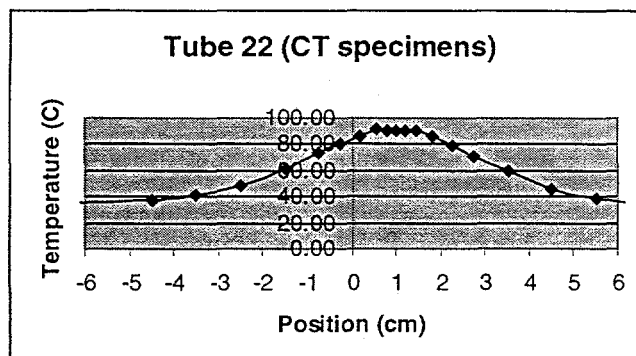


Figure 5. Compact tension center temperature vs location along holder length.

Very detailed checking calculations were done as part of the Quality Assurance process to make sure all of the steps in calculating these detailed sample temperatures are accurate. Examples included checking the input provided for the LAHET power density calculations, checking the process of converting the LAHET output to the power densities needed for each sample material at each node position, checking the detailed sample temperature calculations for all of the high to low power density locations in the two types of sample tubes, checking the calculations that used thermocouple data and calculations to estimate the gap resistances between the sample holders and cover plates, and making sure the output summaries were accurate. Checking calculations included checking the methods used, doing hand calculations to check the detailed model calculations, and checking the mapping of information for input and output use.

Conclusions

Sample temperatures were calculated for all sample locations for the 18C capsule located behind the tungsten neutron source. Gap resistances between sample holders and cover plates were evaluated using thermocouple data vs calculations with zero gap resistance to best determine the nominal gap resistance that was used in the sample temperature calculations. Sample temperatures are

relatively cool in this capsule because of the lower power densities that result from the position behind the tungsten neutron source. Temperatures were calculated at 21 locations along the sample holder length with fine resolution in the region near beam centerline where peak temperatures occur. We will next use similar methods to calculate temperatures for the 17A capsule that contains window materials and has higher power densities because it is located in the first position behind the window and before the tungsten neutron source.

Acknowledgments

This program benefited from a large collaboration involving scientists and engineers from numerous groups at Los Alamos National Laboratory as well as a materials working group consisting of representatives from Pacific Northwest National Laboratory, Oak Ridge National Laboratory, Sandia Livermore National Laboratory, Lawrence Livermore National Laboratory, Savannah River Technology Center and Brookhaven National Laboratory. We are indebted to all participants.

References

1. Maloy, S.A., Sommer, W.F., Brown, R.D., Roberts, J.E., Eddleman, J., Zimmermann, E. and Willcutt, G. Materials for Spallation Neutron Sources, Ed. By M.S. Wechsler, L.K. Mansur, C.L. Snead and W.F. Sommer, The Minerals, Metals & Materials Society, (1998), pp. 131-138.
2. Prael, R.E. and Lichtenstein, H., User Guide to LCS: The LAHET Code System, LA-UR 89-3014, Radiation Transport Group, Los Alamos National Laboratory, Los Alamos, NM, (1989).
3. Prael, R.E. and Madland, D.G, LAHET Code System Modifications for LAHET 2.8, LA-UR-95-3605, Los Alamos National Laboratory, Los Alamos, NM, (1995).
4. Maloy, S.A. and Sommer, W.F., Proceedings of the Topical Meeting on Nuclear Applications of Accelerator Technology, American Nuclear Society, (1997), pp. 58-61.